Ocean Engineering 288 (2023) 116141

Contents lists available at ScienceDirect

Ocean Engineering

journal homepage: www.elsevier.com/locate/oceaneng

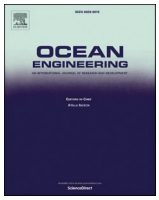

Understanding the effect of design parameters on the filtration efficiency of trawls intended for commercial harvesting of zooplankton

Eduardo Grimaldo [a,b,*], Bent Herrmann [a,b,c], Enis N. Kostak [b], Jesse Brinkhof [a,b]

[a] SINTEF Ocean, Department of Fisheries Technology, Brattørkaia 17C, 7010, Trondheim, Norway
[b] UiT the Arctic University of Norway, Norwegian College of Fishery Science, Breivika, 9037, Tromsø, Norway
[c] Technical University of Denmark, Section for Fisheries Technology, Institute for Aquatic Resources, Willemoesvej 2, 9850, Hirtshals, Denmark

ARTICLE INFO

Handling editor: Prof. A.I. Incecik

Keywords:
Fishery
Trawl
Zooplankton
Flow
Drag
Filtration efficiency
Calanus spp

ABSTRACT

A major challenge for the aquaculture sector is access to sustainable and cost-effective raw materials for feed. Copepods (*Calanus* spp.) have potential to meet this need for large volumes of marine raw materials to enable sustainable growth of aquaculture production worldwide. However, the lack of an energy- and catch-efficient trawl technology has limited the development of this fishery in the Northeast Atlantic. Therefore, the goal of this study was to develop a next generation trawl for harvesting zooplankton that was less energy demanding and more catch efficient than current trawl designs. We assessed the filtration efficiency of low porosity nets with different solidities and studied the effects of design parameters (mesh opening, twine thickness, porosity, taper angle) at various flow velocities in a flume tank. We found that the filtration efficiency for a square meshed net increased with increasing velocity and decreasing solidity and taper angle. A large open area ratio (the ratio between the open netting area and the net's mouth area) improved the filtration efficiency at towing velocities below 0.5 ms^{-1}. These results provided an indication of the initial filtration efficiency of the net designs (i.e., before any clogging occurs) but not of the sustained filtration efficiency.

1. Introduction

Food produced from fisheries and ocean aquaculture currently accounts for 17% of the global production of edible meat (Costello et al., 2020). Therefore, a major future challenge is to cultivate the ocean in an environmentally and economically sustainable way while making seafood production less dependent on existing human food chains. By utilising marine species and fractions deemed unsuitable for human consumption, the dependency on edible fish (i.e., anchoveta) and land-based feed ingredients (i.e., soybeans) for aquaculture feed will decrease (Demets and Foubert, 2021). Due to the increasing demand for global marine ingredients (i.e., fish oil, fish meal) as feed for aquaculture and human consumption, there is a growing need for suitable sources that can provide omega-3-rich oil, protein, and other bioactive compounds (Lenihan-Geels et al., 2013; Hua et al., 2019).

The ocean is home to a plethora of species, especially in lower trophic levels, that are either not harvested or only marginally utilized (FAO, 2020). In the Nordic seas, zooplankton is a key component in the energy transfer from primary producers to higher trophic levels. The copepod *Calanus finmarchicus* is one of the most found species of zooplankton in the subarctic waters of the North Atlantic and is a key species in the North Atlantic food web, as it provides sustenance for a variety of marine organisms, including fish, shrimp, and whales (Skjoldal, 2005). The current estimate of *Calanus* spp. biomass is 290 million metric tonnes (MT) (Broms, 2016), of which *C. finmarchicus* is dominant (Aksnes and Blindheim, 1996).

Although the fishery for *Calanus* spp. was opened for commercial operations in 2017, with a total allowable catch of 254,000 MT in 2021, the annual catches remain relatively small (<1200 MT). In 2021, the *Calanus* spp. landings reached 1156 MT (Norwegian Directorate of Fisheries, 2022), reflecting the lack of a catch-efficient and cost-efficient fishing gear. Currently, the fishery uses fine-meshed trawls (~500 μm bar length) with a low taper angle (5°) and large mouth openings (up to 120 m^2) to harvest *Calanus* spp. However, these trawls prove to be impractical for large-scale zooplankton harvesting because of their very high towing resistance and limited catch efficiency, which translate to high fuel consumption and consequent high CO_2 emission. At 1 knot towing speed (0.5 ms^{-1}), these trawls have a tow resistance (drag) of approximately 10 tons. Depending on the *Calanus* densities, these trawls can reach catch rates of up to 1 MT per hour. However, catch rates normally fluctuate between 0.2 and 0.3 MT per hour (Grimaldo and

* Corresponding author. SINTEF Ocean, Department of Fisheries Technology, Brattørkaia 17C, 7010, Trondheim, Norway.
E-mail address: eduardo.grimaldo@sintef.no (E. Grimaldo).

https://doi.org/10.1016/j.oceaneng.2023.116141
Received 6 July 2023; Received in revised form 21 September 2023; Accepted 21 October 2023

Nomenclature

u_0	the average velocity component in the direction of U of the flow that passes through the net cone; for a net cone, u_0 equals the average velocity across the mouth (m/s)
U	undisturbed flow (towing) velocity some distance upstream of the net (m/s)
A_o	area of the net mouth; $A_o = \pi D_c^2/4$
a_o	Open area of a square mesh
D_c	large diameter of cone section = net mouth diameter
d_c	small diameter of net cone
L	length of the net (only the conical section)
L_s	length of the cone wall
d	twine diameter (μm)
m	mesh bar length (μm)
w	mesh opening (μm)
b	bar length
a_o	open area of a square mesh
α	taper angle
β	porosity
A_S	surface area of net cone
R_A	open area ratio = ratio between the open mesh area and the mouth area; $R = \beta/\sin(\alpha)$
S_n	solidity; $S_n = 1 - \beta$
ρ	density
R_e	Reynolds number
F_D	drag force (N)
C_D	drag coefficient
C_N	normal force coefficient
F	filtration efficiency; $F = u_0/U$
F_i	initial filtration efficiency
F_s	sustained filtration efficiency

Gjøsund, 2012).

For nets and trawls with high solidity that are specifically designed for harvesting *Calanus* spp., both the filtration efficiency and towing resistance strongly depend on the design parameters and towing speed. In particular, the Reynolds number dependency may be dramatic for fine-meshed trawls compared to more traditional trawls, and care must be taken when assessing the flow conditions in such trawls. The flow through the main part of traditional fish trawls is usually considered to be uniform and undisturbed by the trawl. The porosity (β) of such trawls is relatively high (typically $\beta > 0.8$), and the Reynolds number based on twine diameter (Re_d) is in the order of 10^3–10^4. In trawls intended for catching *C. finmarchicus*, the mesh size and twine thickness are both in the order of 10^{-4} m, $\beta \approx 0.5$, and Re_d is 10^0–10^2. Due to the close spacing between the twines, the entire flow field, filtered volume, and drag of such nets depend strongly on the net parameters (twine thickness, mesh size, taper angle) and towing velocity.

Breddermann (2017) investigated the flow through nets widely used for plankton sampling (i.e., Multiple Opening/Closing Net and Environmental Sensing System MOCNESS, ring net California Cooperative Oceanic Fisheries Investigations, Multinet Midi, Bongo net, Apstein nets) and quantified the effect of different design parameters on filtration efficiency. The results in that study showed that the filtration efficiency of the meso-zooplankton nets do not differ largely above a towing velocity of 0.5 ms^{-1}. Furthermore, he found that the filtration efficiency of these nets decreases with a decrease of the mesh width and a decrease of the porosity. Gjøsund and Enerhaug (2010) and Gjøsund (2012) described correlations for the flow through and forces on tapered net sections. Based on pressure drop and streamline deflection through porous screens, they presented parametric examples for the filtration efficiency (F) and drag on conical nets. The model allows easy assessment of the effect of varying mesh opening (m), twine thickness (d), porosity (β), taper angle (α), and flow velocity (U). For a tapered net, the pressure drop through the net panels defines the degree to which the flow is blocked, and the pressure drop is primarily a function of the ratio between the total open mesh area of the section and the inlet area of the section (Gjøsund and Enerhaug, 2010). The filtration efficiency F is defined as the ratio between the average velocity U across the net mouth (D_c) and the velocity of the net through the water (u_0) (i.e., the towing velocity through quiescent water) (Grimaldo and Gjøsund, 2012). A net panel or a trawl section always causes some blocking of the flow. However, the blocking only becomes noticeable if the panel has both sufficiently low porosity (small mesh opening, high solidity) and steep taper angle (Valdemarsen et al., 2011).

Generally, the towing resistance of low porosity nets, like plankton nets, increases with the tow velocity squared (Paschen and Winkel, 2000; Gjøsund and Enerhaug, 2010; Breddermann, 2017). This is rarely a problem for small sampling nets, but it can be extremely important for the fuel efficiency of large commercial plankton trawls. One of the main concerns for designing commercial plankton trawls is finding the balance between maximizing the trawl mouth area (to increase catch efficiency) and the reducing total drag (to reduce fuel consumption) (Grimaldo and Gjøsund, 2012). Earlier studies assessing the effect of cutting rate and taper angle (Liu et al., 2021; Nyatchouba Nsangue et al., 2022, 2023; Wan et al., 2019; Zhou et al., 2015) and netting solidity (Tang et al., 2017, 2019; Thierry et al., 2020) on the drag of krill trawls are mostly based on trawls with solidities smaller than 0.5.

In this study we assess the effect of these design parameters in nets with solidities larger than 0.5. The objective was to create the base for developing a next generation *Calanus* spp. trawl being less energy demanding and having higher catch efficient than current designs. To do so, we measured the filtration efficiency of different plankton trawls and tested the effects of the trawl's design parameters (mesh opening, twine thickness, porosity, and taper angle) on the total drag under different flow conditions. We specifically addressed the following questions: i) what is the filtration efficiency of different designs of *Calanus* spp. nets and ii) which combination of mesh opening, solidity, and taper angle provides the best filtration efficiency at specific flow speeds?

2. Materials and methods

The experiments were carried out at the SINTEF flume tank in Hirtshals, Denmark on June 2–3, 2022. The dimensions of the measuring section of the tank were 21.3 m (length) × 8.0 m (width) × 2.7 m (depth), with a total volume of ~460 m^3. The maximum speed applicable to the water was 1.0 ms^{-1}. The flume tank had a bottom conveyor belt that runs at the same speed as the nominal water velocity, thereby avoiding a bottom boundary layer.

2.1. Net models

Net models were made in scale 1:1, with full scale plankton nets built from polyamide 6.6 monofilament (KC Denmark A/S, Silkeborg, Denmark). Each model consisted of a conical shaped net with a hoop attached to the opening. The hoop was made of polyamide and had a diameter (D_c) of 1.0 m (Fig. 1). The function of the hoop was to prevent the opening from collapsing and to ensure an evenly distributed load around the opening circumference.

Eight combinations of taper ratio and solidity were tested. All net models had the same circular opening. Four net models had different nominal mesh sizes (w = 250, 500, 750, and 1000 μm) and similar 5-degree taper angle (α). The actual mesh sizes of the 250, 500, 750, and 1000 μm nets were 194, 440, 656, and 899 μm, respectively. The other

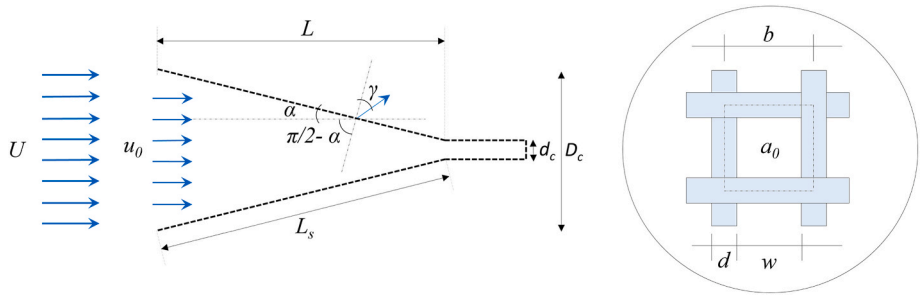

Fig. 1. Sketch of flow through a conical net with taper angle α and filtration efficiency $F = u_0/U$; the angle γ describes the streamline deflection through the net wall.

four net models had different taper angles (10°, 15°, 20°, and 30°) and similar nominal 750 μm mesh sizes. Table 1 lists specifications of the net models.

Design parameters were estimated for all net models using the following equations:

$$\text{Taper angle} : \alpha = tan^{-1}(D_c - d_c) / 2L_s) \tag{1}$$

$$\text{Surface area of the trawl net} : A_s = \frac{\pi L_c (D_c - d_c)}{2} \tag{2}$$

$$\text{Open area of a square mesh} : a_0 = w^2 \tag{3}$$

$$\text{Porosity (for square meshes)} : \beta = \frac{w^2}{b^2} = \frac{w^2}{(w+d)^2} \tag{4}$$

$$\text{Solidity} : S_n = 1 - \beta = 1 - \frac{1}{\left(1 + \frac{d}{w}\right)^2} \tag{5}$$

$$\text{Open ratio area } R_A = \beta / \sin(\alpha) \tag{6}$$

2.2. Test procedure

The net models were connected to the main towing wire with four bridles (each 2 m long) attached to the hoop. The experiments involved measuring water flow and drag of the nets. The flow rate was measured using a 2-component electromagnetic current meter (Model 802, Valeport Limited, Devon TQ9, 5 EW, UK) at a frequency of 10 Hz over a period of 300 s (5 min) and with a measurement accuracy of ±1%. The velocity components in the longitudinal direction of the tank (*x*-component) and horizontally across it (*y*-component) were measured. The *y*-component of the velocity was consistently very low and negligible while the *x*-component of the flow rate was used for assessing filtration efficiencies. The flow in the tank is considered reproducible between trials, with the same nominal flow rate (setpoint speed) in the tank. The actual flow rate measured with the electromagnetic current meter is usually considered equal to the "setpoint speed" in the main part of the tank. Control measurements were made to validate the difference between actual flow rate and the setpoint flow speed (i.e., for undisturbed flow). The flow rates were measured at four points in front of the nets (Fig. 2) using the electromagnetic current flow sensor mounted on a vertical rod. The undisturbed velocity (U) was measured at position 1, and the average velocity component in the direction of U of the flow that passes through the net (u_o) was the average of the velocities measured at positions 2, 3, and 4 (Fig. 2). Mean value and standard deviation were calculated at each measurement point. The tests were carried out at a setpoint flow speed of 0.31, 0.51, 0.72, and 0.98 ms^{-1}, which correspond to tow speeds between 0.60 and 1.91 knots. The drag measurements were acquired using a submersible miniature S-beam load cell (Model LSB210 FUTEK, CA 92618 USA) attached to the single bridle. The load cell capacity was 445 N and its accuracy was 0.2% of the rate output. Each net was tested individually by increasing the speed, respectively, and only horizontal towing direction flow velocity was considered in this study (see Fig. 3).

Table 1
Net model data. Main dimensions and characteristics of the net models: w, d, L_s, L, and α are actual measurements, and β was estimated using Eq. (4) and S_n using Eq. (5).

Net model	w/d (μm)	L_s (mm)	L (mm)	α	β	S_n
A1	194/198	4400	4380	5.2°	0.23	0.77
A2	440/345	4400	4380	5.2°	0.34	0.66
A3	656/318	4400	4380	5.2°	0.46	0.54
A4	899/514	4400	4380	5.2°	0.43	0.57
B3	656/318	2270	2230	10.2°	0.46	0.54
C3	656/318	1460	1400	15.9°	0.46	0.54
D3	656/318	1200	1130	19.5°	0.46	0.54
E3	656/318	780	670	30.9°	0.46	0.54

2.3. Filtration efficiency

The filtration efficiency (F) is defined as the ratio between the average flow that passes through the net (u_o) (measured at positions 2, 3, and 4) and the undisturbed velocity (U) that was measured at position 1 (Eq. (7)).

$$F = \frac{u_0}{U} \tag{7}$$

In Eqs. (8) and (9), C_D is the estimated overall drag coefficient, F_D is the measured overall drag force, A_0 is the mouth area, and ρ is density:

$$C_D = \frac{F_D}{1/2\rho U^2 A_0} \tag{8}$$

$$F_D = \frac{1}{2}\rho U^2 A_o C_D \tag{9}$$

We compared the filtration efficiency (F) of our net models (Table 1) with measurements from Enerhaug (2005), who tested eight different nets at three current velocities (0.13, 0.58, and 0.83 ms^{-1}) in the same flume tank in Hirtshals, Denmark. Those nets were made of synthetic monofilament fabric with square mesh openings of $143 \leq w \leq 950$ mm, twine thicknesses of $105 \leq d \leq 315$ mm, and porosities of $0.23 \leq \beta \leq$

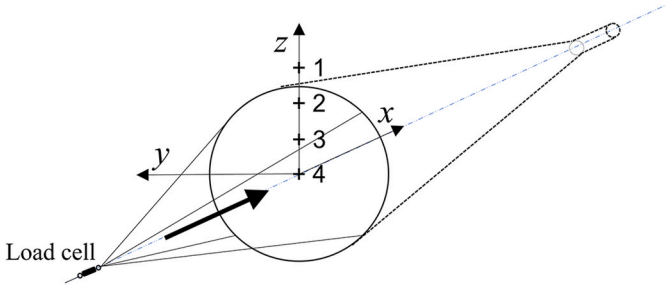

Fig. 2. Measurements points of water speed.

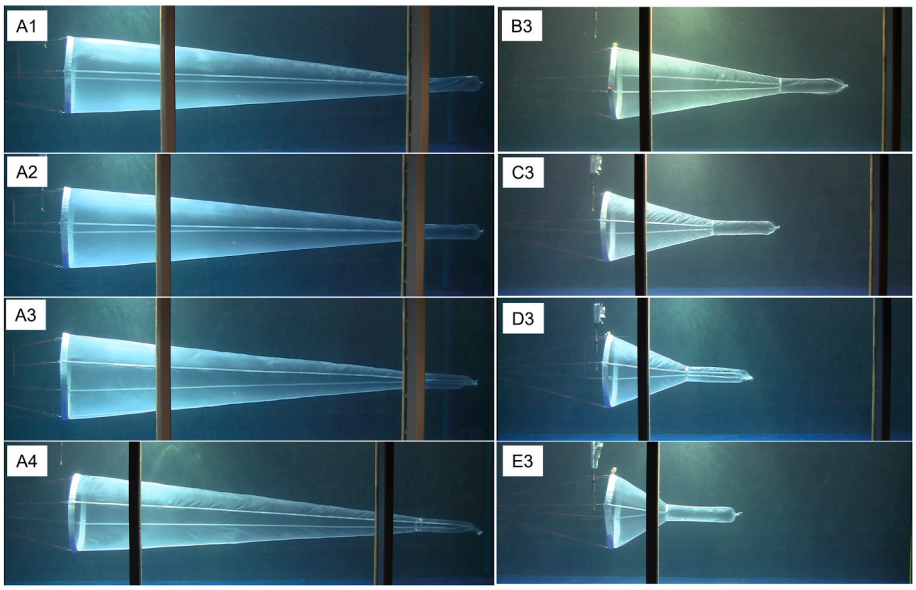

Fig. 3. Images of net models in the flume tank.

0.57 mm. All nets had a mouth diameter (D_c) of 0.8 m, taper angle (α) varied from 4.5° to 15°, and lengths of the nets (L_s) varied from 1.5 to 5.1 m. Finally, we compared our results to the parametric models described by Gjøsund and Enerhaug (2010).

2.4. Modelling the effect of design parameters on drag coefficient (C_D) and filtration efficiency (F)

We used the function "*lm*" in the statistical tool *R* (version 4.3.1) for a multi-parameter linear regression for the effect of gear design parameters on respectively drag coefficient and filtration efficiency. As starting point for the analysis, we considered models on the following form:

$$C_D = q_0 + q_1 w + q_2 d + q_3 \beta + q_4 L_s \quad (10)$$

$$F = q_0 + q_1 w + q_2 d + q_3 \beta + q_4 L_s + q_5 U \quad (11)$$

For all our designs there is a constant relation between taper angle α and the length L_s given by Eq. (1). Therefore, Eqs. (10) and (11) only consider L_s. Beside design parameters *w, d, β* and L_s Eq. (11) also considers the undisturbed flow velocity U because and initial evaluation showed it necessary. Based on Eqs. (10) and (11) stepwise elimination of nonsignificant parameters ($p > 0.05$) was applied to find the best model for respectively C_D and F. The coefficient of determination (r^2-value) was used to judge the resulting models.

3. Results

3.1. Effect of flow speed (U) on the total drag force (F_D) for all net models

Generally, the difference in the total F_D between net designs was larger as U increased. At low U (0.31 ms^{-1}), F_D varied between 37.4 N (net model D3) and 64.3 N (net model A1). At high U (0.98 ms^{-1}), F_D varied between 332.5 N (net model D3) and 617.4 N (net model A1) (Table 2). For all net models, F_D increased with U squared (Fig. 4, Table 3).

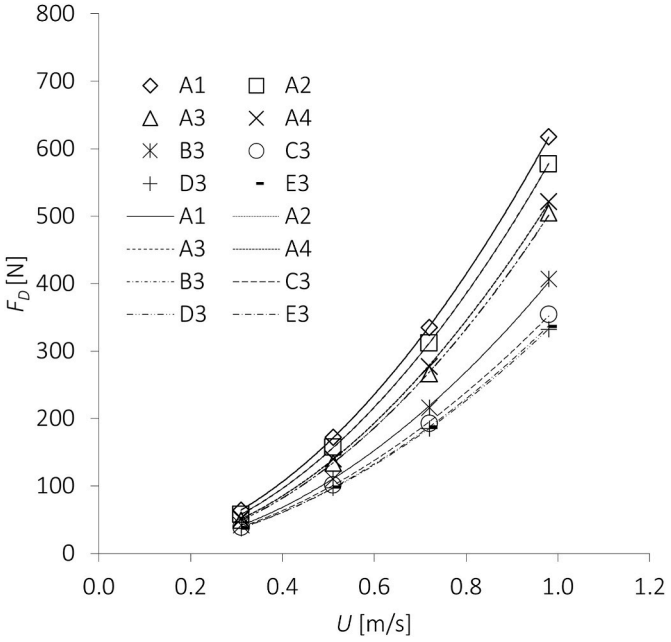

Fig. 4. Effect of water speed (U) on the total drag (F_D) for all net models.

Table 2
Flow-induced drag force (F_D) in Newtons for flow speeds $U = 0.31$, 0.51, 0.72, and 0.98 ms^{-1} The values for net models with equal solidity ($S_n = 0.54$) are in bold type.

U (ms^{-1})	A1	A2	A3	A4	B3	C3	D3	E3
	$\alpha = 5.2°$ $S_n = 0.77$	$\alpha = 5.2°$ $S_n = 0.66$	$\alpha = 5.2°$ $S_n = 0.54$	$\alpha = 5.2°$ $S_n = 0.57$	$\alpha = 10.2°$ $S_n = 0.54$	$\alpha = 15.9°$ $S_n = 0.54$	$\alpha = 19.5°$ $S_n = 0.54$	$\alpha = 30.9°$ $S_n = 0.54$
0.31	64.3	57.8	**49.4**	51.0	**41.7**	**39.0**	**37.4**	**37.5**
0.51	172.4	157.5	**133.9**	140.2	**110.3**	**101.8**	**97.2**	**98.6**
0.72	335.2	311.5	**266.6**	276.9	**216.1**	**193.0**	**184.9**	**187.2**
0.98	617.4	577.4	**505.1**	521.6	**406.8**	**354.3**	**332.5**	**336.2**

Table 3
Regression fit describing the effect of water speed (U) on the total drag (F_D) for all net models shown in Fig. 4.

Net	Equation	r^2
A1	$F_D = 641.81\ U^{1.9621}$	>0.9999
A2	$F_D = 601.60\ U^{1.9977}$	>0.9999
A3	$F_D = 522.16\ U^{2.0182}$	0.9999
A4	$F_D = 541.51\ U^{2.0161}$	0.9999
B3	$F_D = 418.71\ U^{1.9750}$	0.9998
C3	$F_D = 366.03\ U^{1.9114}$	0.9998
D3	$F_D = 345.85\ U^{1.8970}$	>0.9999
E3	$F_D = 350.77\ U^{1.9038}$	>0.9999

3.2. Effect of taper angle (α) on total drag force (F_D)

Net models with large α were consistently associated with low F_D, meaning that F_D decreased as α increased. At low U (0.31 ms^{-1}), the measured F_D varied between 37.4 and 49.4 N for the 20° and 5° net models, respectively (Table 4). Power regression curves described the experimental data very well ($r^2 > 0.9$) (Table 4) and showed that the relationship between α and F_D was stronger as U increased (Fig. 5). At high U (0.98 ms^{-1}), F_D varied between 332.5 and 505.1 N (Table 4).

3.3. Effect of taper angle (α) on drag coefficient (C_D)

Generally, C_D decreased as α increased. At $\alpha = 5.2°$, C_D was similar for all U values. C_D varied between 1.351 at U of 0.31 ms^{-1} and 1.383 at U of 0.98 ms^{-1}. As α increased, the difference in C_D between different U speeds was larger. For the net model with 30.9° α (net model E3), for instance, C_D was 0.891 at U of 0.98 ms^{-1} and 0.993 at U of 0.31 ms^{-1} (Fig. 6, Table 5). The effect of α on C_D was well described by a power regression ($r^2 > 0.9$) (Fig. 6, Table 6).

3.4. Effect of mesh opening (w) on the total drag force (F_D)

F_D decreased as w increased. The effect of w on F_D was well described by a power regression ($r^2 > 0.86$) (Fig. 7, Table 7). According to the regression model, increasing U led to larger F_D. At low U (0.31 ms^{-1}), F_D varied between 49.3 N and 64.3 N, with the highest drag for the 250 μm mesh size net. At high U (0.98 ms^{-1}), F_D varied between 502.1 N and 617.4 N, again with the highest drag for the 250 μm mesh size net.

3.5. Effect of mesh opening (w) on drag coefficient (C_D)

C_D decreased as w increased. The relationship was well-described by power regression curves, which fitted the experimental data well ($r^2 > 0.86$) (Fig. 8, Table 8). The same trend was found for all net models with equal solidity ($S_n = 0.54$). Increased U marginally modified the C_D.

3.6. Filtration efficiency (F) for all nets

Table 9 lists the F estimated for all net models tested using Eq. (7). None of the net models reached 100% F (i.e., $F = 1.0$). Power regression curves described the experimental data very well ($r^2 > 0.88$) (Fig. 9, Table 10). F increased with increasing U for all net models and was highest at 0.98 ms^{-1}. At low U (0.31 ms^{-1}), F varied between 0.74 and 0.84, and net models A2, A3, and A4 had better F than the other net models. At high U, this difference was smaller for almost all net models except for model E3. The poorest F was observed for model E3 which had the largest α (Fig. 9, Table 10). Generally, large α lead to low F. Compared to earlier results (Enerhaug, 2005) for nets with $S_n = 0.53$, our results (especially those for net models with $S_n = 0.54$), were well in agreement and showed similar patterns (Fig. 9).

Table 4
Regression fit describing the effect of taper angle (α) on the total drag (F_D) for speeds (U) of 0.31, 0.51, 0.72, and 0.98 ms^{-1} for net models with equal solidity ($S_n = 0.54$) shown in Fig. 5.

Velocity	Equation	r^2
$U = 0.31$ ms^{-1}	$F_D = 61.86\ \alpha^{-0.160}$	0.9202
$U = 0.51$ ms^{-1}	$F_D = 172.13\ \alpha^{-0.181}$	0.9029
$U = 0.72$ ms^{-1}	$F_D = 359.44\ \alpha^{-0.211}$	0.9133
$U = 0.98$ ms^{-1}	$F_D = 723.14\ \alpha^{-0.245}$	0.9376

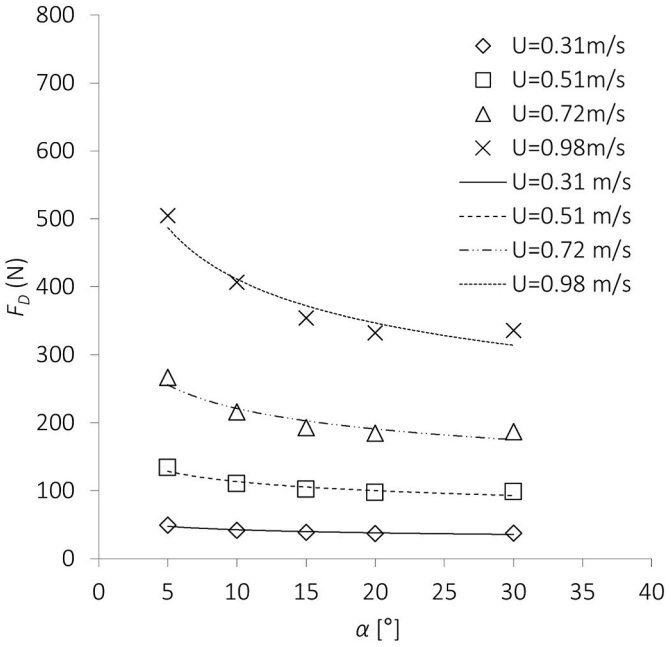

Fig. 5. Effect of taper angle (α) on the total drag (F_D) for speeds (U) of 0.31, 0.51, 0.72, and 0.98 ms^{-1} for net models with equal solidity ($S_n = 0.54$).

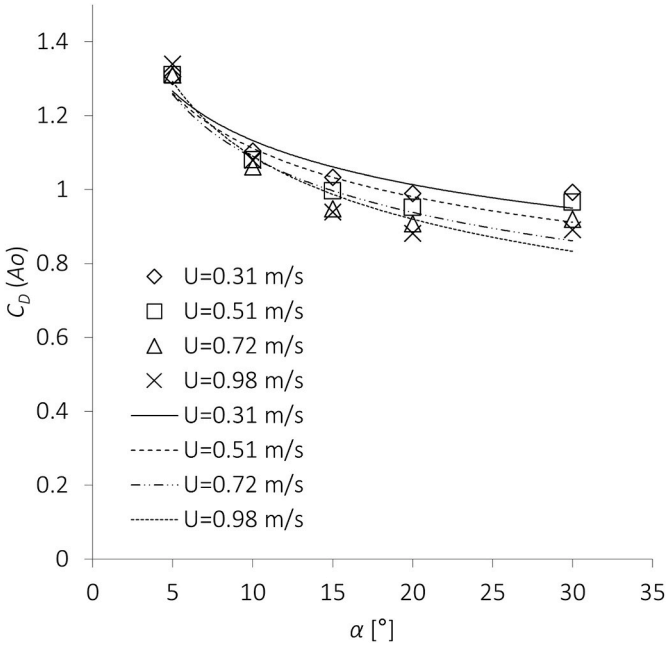

Fig. 6. Effect of taper angle (α) on the drag coefficient (C_D) for speeds (U) of 0.31, 0.51, 0.72, and 0.98 ms^{-1} for net models with equal solidity ($S_n = 0.54$) and different taper angle α.

Table 5
Effect of taper angle (α) on drag coefficient (C_D) for speeds (U) of 0.31, 0.51, 0.72, and 0.98 ms^{-1} In bold are the values for net models with equal solidity (Sn = 0.54).

U (ms^{-1})	A1	A2	A3	A4	B3	C3	D3	E3
	$\alpha = 5.2°$	$\alpha = 5.2°$	$\alpha = 5.2°$	$\alpha = 5.2°$	$\alpha = 10.2°$	$\alpha = 15.9°$	$\alpha = 19.5°$	$\alpha = 30.9°$
0.31	1.705	1.533	**1.351**	1.306	**1.104**	**1.033**	**0.990**	**0.993**
0.51	1.688	1.542	**1.373**	1.310	**1.080**	**0.996**	**0.952**	**0.966**
0.72	1.647	1.530	**1.360**	1.310	**1.062**	**0.948**	**0.908**	**0.920**
0.98	1.637	1.531	**1.383**	1.339	**1.079**	**0.939**	**0.882**	**0.891**

Table 6
Regression fit describing the effect of taper angle (α) on the drag coefficient (C_D) for speeds (U) of 0.31, 0.51, 0.72, and 0.98 ms^{-1} for net models with equal solidity ($S_n = 0.54$) and different α shown in Fig. 6.

Velocity	Equation	r^2
$U = 0.31$ ms^{-1}	$C_D = 1.6392\ \alpha^{-0.160}$	0.9202
$U = 0.51$ ms^{-1}	$C_D = 1.6853\ \alpha^{-0.181}$	0.9029
$U = 0.72$ ms^{-1}	$C_D = 1.7657\ \alpha^{-0.211}$	0.9133
$U = 0.98$ ms^{-1}	$C_D = 1.9174\ \alpha^{-0.245}$	0.9376

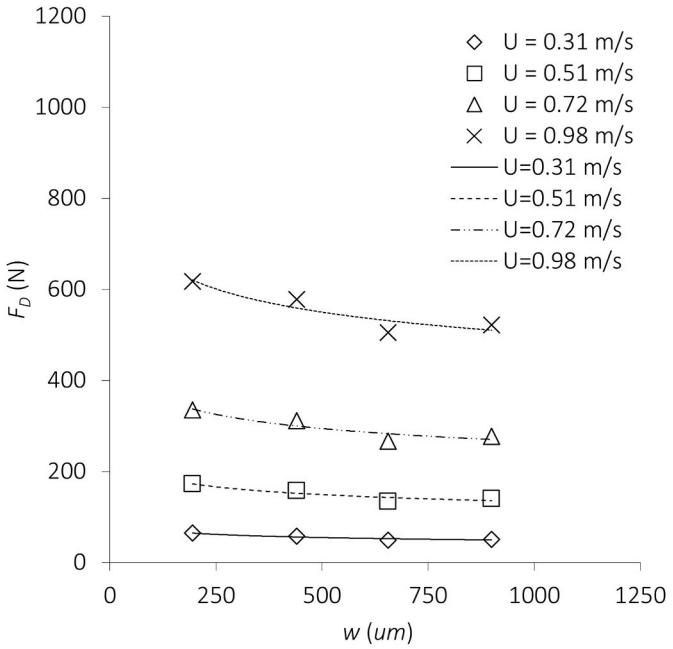

Fig. 7. Effect of mesh opening (w) on the total drag force (F_D) for speeds (U) of 0.31, 0.51, 0.72, and 0.98 ms^{-1} for net models with equal solidity ($S_n = 0.54$).

3.7. Filtration efficiency (F) as function of open area ratio (R_A)

For the net models with equal solidity ($S_n = 0.54$), Table 11 and Fig. 10 show the F as a function of R_A for U of 0.31, 0.51, 0.72, and 0.98 ms^{-1}. None of the net models reached 100% F. Power regression curves fitted to the experimental data ($r^2 > 0.62$) generally showed that F was positively correlated with R_A, with F increasing as function of R_A. Higher U also led to higher F for all cases (Fig. 10, Table 12). Compared to

Table 7
Regression fit describing the effect of mesh opening (w) on the total drag force (F_D) for speeds (U) of 0.31, 0.51, 0.72, and 0.98 ms^{-1} shown in Fig. 7.

Velocity	Equation	r^2
$U = 0.31$ ms^{-1}	$F_D = 185.41\ w^{-0.192}$	0.9088
$U = 0.51$ ms^{-1}	$F_D = 454.02\ w^{-0.175}$	0.8705
$U = 0.72$ ms^{-1}	$F_D = 822.20\ w^{-0.162}$	0.8648
$U = 0.98$ ms^{-1}	$F_D = 1357.9\ w^{-0.142}$	0.8693

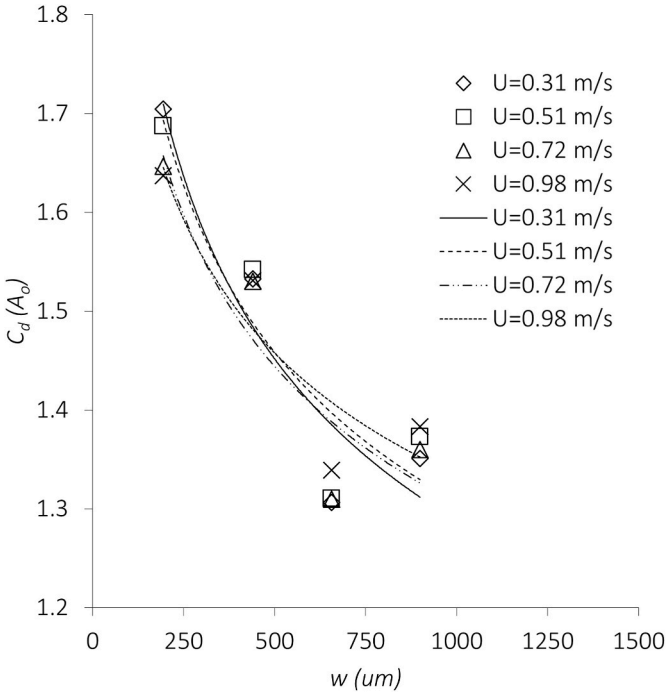

Fig. 8. Effect of mesh opening (w) on the drag coefficient (C_D) for speeds (U) of 0.31, 0.51, 0.72, and 0.98 ms^{-1}.

earlier results (Enerhaug, 2005) for nets with $S_n = 0.53$, our results, especially those for net models with $S_n = 0.54$, were well in agreement and showed similar patterns (Fig. 10).

3.8. Filtration efficiency (F) as function of taper angle (α)

The F decreased as α increased, and the effect of α on F was described by a power regression ($r^2 > 0.61$) (Fig. 11, Table 13). According to the regression model, increasing U improved the F. At low U (0.31 ms^{-1}), net models with low α (5°) had better F than nets with high α values. A similar pattern was observed at high U (0.98 ms^{-1}). None of the net models reached a 100% F ($F = 1.0$).

Table 8
Regression fit describing the effect of mesh opening (w) on the drag coefficient (C_D) for speeds (U) of 0.31, 0.51, 0.72, and 0.98 ms^{-1} for net models with equal solidity ($S_n = 0.54$) shown in Fig. 8.

Velocity	Equation	r^2
$U = 0.31$ ms^{-1}	$C_D = 4.9131\ w^{-0.192}$	0.9088
$U = 0.51$ ms^{-1}	$C_D = 4.4450\ w^{-0.175}$	0.8705
$U = 0.72$ ms^{-1}	$C_D = 4.0388\ w^{-0.162}$	0.8648
$U = 0.98$ ms^{-1}	$C_D = 3.6004\ w^{-0.142}$	0.8693

Table 9
Filtration efficiency F (mean value) for four flow speeds (U).

U (ms^{-1})	A1	A2	A3	A4	B3	C3	D3	E3
0.31	0.796	0.806	0.839	0.818	0.743	0.781	0.752	0.745
0.51	0.874	0.895	0.885	0.901	0.826	0.858	0.835	0.806
0.72	0.914	0.922	0.915	0.926	0.878	0.890	0.879	0.844
0.98	0.946	0.958	0.959	0.956	0.938	0.946	0.928	0.879

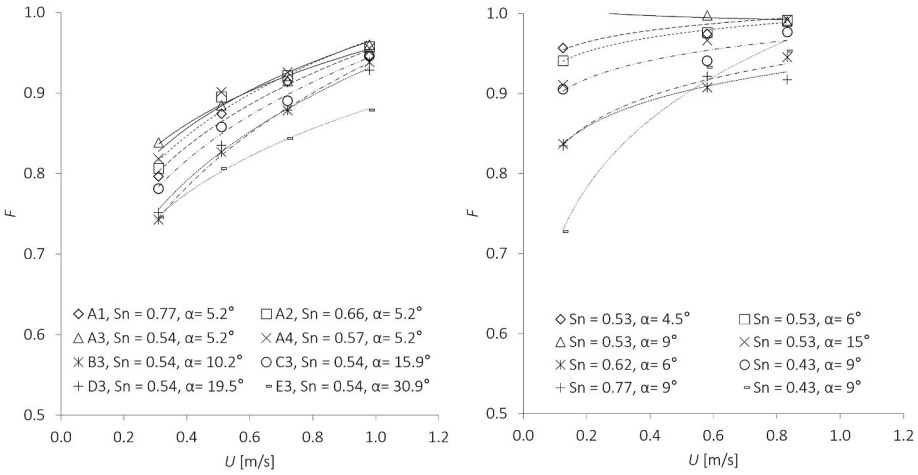

Fig. 9. Left: filtration efficiency ($F = u/U$) of all net models and speeds (U). Right: results from Enerhaug (2005).

Table 10
Regression fit describing the filtration efficiency ($F = u/U$) of all net models as function of speeds (U) (plotted in Fig. 9).

Net	Equation	r^2
A1	$F = 0.9560\ U^{0.1497}$	0.9840
A2	$F = 0.9681\ U^{0.1463}$	0.9622
A3	$F = 0.9569\ U^{0.1148}$	0.9903
A4	$F = 0.9666\ U^{0.1327}$	0.9579
B3	$F = 0.9415\ U^{0.2007}$	0.9987
C3	$F = 0.9471\ U^{0.1618}$	0.9903
D3	$F = 0.9345\ U^{0.1816}$	0.9949
E3	$F = 0.8833\ U^{0.1426}$	0.9977

3.9. Effect of design parameters on drag coefficient (C_D) and filtration efficiency (F)

Using stepwise elimination with Eq. (10) as starting point the following model (Eq. (12) and Table 14) was obtained for the influence of design parameters on $\boldsymbol{C_D}$:.

$$C_D = q_0 + q_1 w + q_3 \beta + q_4 L_s \tag{12}$$

The model for C_D (Eq. (12), Table 14) shows that the parameters w, β, and L_S had a significant effect on C_D. Increasing w and β decreases C_D while increasing L_S will increase C_D.

Using stepwise elimination with Eq. (11) as starting point the following model (Eq. (13)) and Table 15) was obtained for the influence of design parameters on $\boldsymbol{F}$:.

$$F = q_0 + q_4 L_s + q_5 U \tag{13}$$

The model for F (Eq. (13), Table 15) shows that the parameters L_S and U had a significant effect on F. Increasing L_S and U increases F.

4. Discussion

In traditional large-meshed, low-solidity fish trawls, the flow is generally believed to be practically unaffected by the trawl's presence, except in the vicinity of and inside the codend. Therefore, research has focused on towing resistance, net geometry, and selectivity performance of meshes and sorting grids in this type of trawl. For nets and trawls of high solidity (e.g., intended for commercial harvesting of marine zooplankton such as *Calanus* spp.), the filtration performance and towing resistance depend strongly on the design parameters and towing speed. In fine-meshed *Calanus* trawls, the mesh size typically is ~0.5 mm, the twine thickness is ~0.2 mm, the solidity is ~0.5, and the flow locally through the meshes can vary dramatically with the Reynolds number in the range of 10^{0}–10^{2}. Therefore, care must be taken when assessing the flow conditions in such trawls, from both theoretical and experimental perspectives.

The towing resistance (hydrodynamic drag F_D) basically increases with the towing velocity squared (Gjøsund and Enerhaug, 2010), which is seldom an issue for small sampling nets, but it can be crucial for the fuel efficiency of larger commercial zooplankton trawls. For the design

Table 11
Filtration efficiency (F) as function of open area ratio (R_A) for flow speeds (U) of 0.31, 0.51, 0.72, and 0.98 ms^{-1}. Net models A3, B3, C3, D3, and E3 had equal solidity ($S_n = 0.54$).

U (ms^{-1})	A1	A2	A3	A4	B3	C3	D3	E3
	$R_A = 2.75$	$R_A = 3.56$	$R_A = 5.16$	$R_A = 4.59$	$R_A = 2.59$	$R_A = 1.74$	$R_A = 1.32$	$R_A = 0.90$
0.31	0.796	0.806	0.839	0.839	0.743	0.781	0.752	0.745
0.51	0.874	0.895	0.885	0.885	0.826	0.858	0.835	0.806
0.72	0.914	0.922	0.915	0.915	0.878	0.890	0.879	0.844
0.98	0.946	0.958	0.959	0.959	0.938	0.946	0.928	0.879

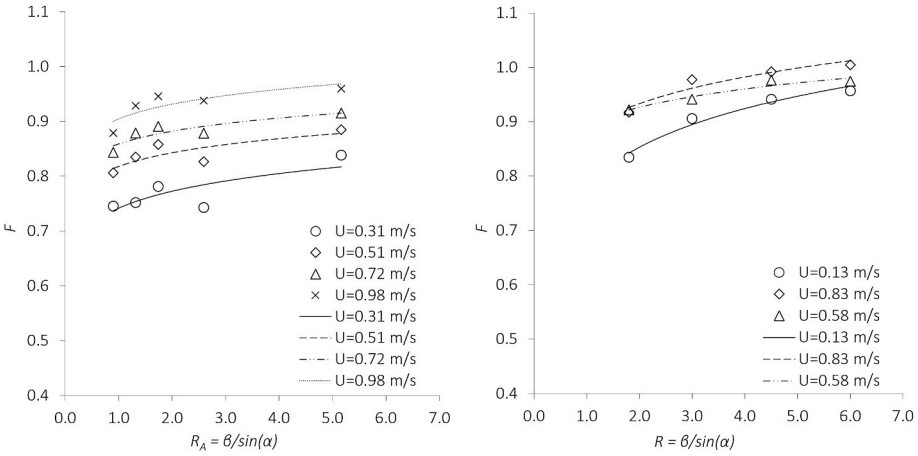

Fig. 10. Filtration efficiency (F) as function of open area ratio (R_A). Left: our measurements for net models with $S_n = 0.54$. Right: results from Enerhaug (2005) for net models with $S_n = 0.53$.

Table 12
Regression fit describing the filtration efficiency (F) as function of open area ratio (R_A) shown in Fig. 10.

Velocity	Equation	r^2
$U = 0.31$ ms^{-1}	$F = 0.7416\ R_A^{0.0589}$	0.6165
$U = 0.51$ ms^{-1}	$F = 0.8176\ R_A^{0.0434}$	0.6641
$U = 0.72$ ms^{-1}	$F = 0.8586\ R_A^{0.0.386}$	0.7793
$U = 0.98$ ms^{-1}	$F = 0.9040\ R_A^{0.0424}$	0.6991

Table 13
Regression fit describing the filtration efficiency (F) as function of taper angle (α) shown in Fig. 11.

Velocity	Equation	r^2
$U = 0.31$ ms^{-1}	$F = 0.8953\ \alpha^{-0.057}$	0.6112
$U = 0.51$ ms^{-1}	$F = 0.9398\ \alpha^{-0.042}$	0.6660
$U = 0.72$ ms^{-1}	$F = 0.9722\ \alpha^{-0.038}$	0.7849
$U = 0.98$ ms^{-1}	$F = 1.0364\ \alpha^{-0.042}$	0.7092

of large commercial zooplankton trawls, key issues such as catch quality, catch- and fuel efficiency, and structural reliability require that the filtration efficiency, towing resistance, and clogging are properly balanced in the design process (Larsen, 2009; Grimaldo and Gjøsund, 2012). In this study, we assessed the hydrodynamic properties of different net designs (i.e., different nominal mesh sizes $250 < w < 1{,}000$, twine diameters $198 < d < 514$, taper angles $5° < \alpha < 30°$, and porosities $0.23 < \beta < 0.46$) to understand and optimize the filtration efficiency of trawls for commercial harvesting of zooplankton in the Northeast Atlantic Ocean.

Our empirical model assessing the effect of design parameters on C_D (Eq. (12)) shows that increasing w and β decreases C_D while increasing L_S will increase C_D. That increasing w and β decreases the drag seem logic as it intuitively would require less force to tow a net with bigger meshes than smaller and because a more porous net would have lower towing resistance than a denser net. Increasing L_S means increasing the total amount of netting which logically would result in increasing the total drag forces. Similarly, Eq. (13) assessing the effect of design parameters on F demonstrates that increasing L_S and U increases F. These results are in agreement with the results of earlier experiments assessing the filtration efficiency of plankton nets (Gjøsund and Enerhaug 2010; Valdemarsen et al., 2011; Breddermann, 2017).

Usually, the open area ratio (R_A) is the only parameter considered when designing plankton nets. R_A is highly dependent on the relationship between solidity (S_n) and porosity (β). A general recommendation is that R_A should be > 3 to have high initial (i.e., before any clogging occurs) filtration efficiency (F_i) (Tranter and Heron, 1967; Gjøsund and Enerhaug, 2010) and >6 to have an additional buffer against clogging and sustained filtration efficiency (F_s) (Harris et al., 2000). Designing nets with high F means first maximizing F_i and then, within those design

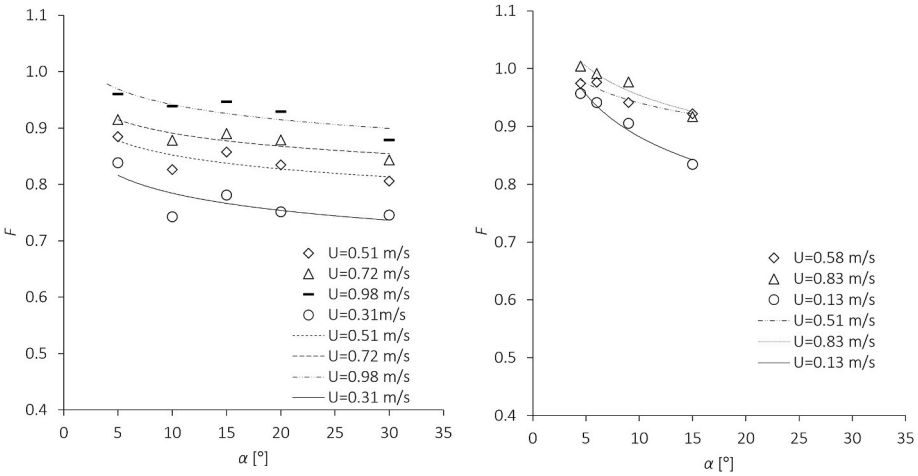

Fig. 11. Filtration efficiency (F) as function of taper angle (α). Left: our measurements for net models with $S_n = 0.54$. Right: results from Enerhaug (2005) for net models with $S_n = 0.53$.

Table 14
Regression fit describing the drag coefficient (C_D) as function of design parameters (Eq. (12)).

Factor	Value	*P-value*
q_0	*1.374e + 00*	<2.00e-16
q_1	−2.796e-04	0.0009
q_3	*−8.088e-01*	0.0009
q_4	*1.240e-04*	<2.00e-16

Table 15
Regression fit describing the drag coefficient (F) as function of design parameters (Eq. (13)).

Factor	Value	*P-value*
q_0	*6.843e-01*	<2.00e-16
q_4	1.612e-05	1.38e-07
q_5	*2.213e-01*	2.93e-15

confines, maximizing F_s. In general, the higher the R_A of a net, the better the F_i and F_s. However, other concerns constrain a net's design, and a sufficient R_A can sometimes be difficult to attain. Our results are in agreement with the literature and showed the best F_i for nets with larger R_A (Fig. 10). However, net selection as a function of design parameters is a trade-off, driven by the conflicting priorities of maximizing R_A, maximizing catch efficiency, and minimizing energy, cost, and effort.

F_i declines sharply when the net's taper angle (α) increases to $> 15^\circ$ (Tranter and Heron, 1967; Gjøsund and Enerhaug 2010). Therefore, we focused on finding the optimal α in the range between 5° to 15° that would translate into a shortening of net length. Our results showed that the highest F_i values were obtained for nets with low α. Net models A2, A3, and A4 all had $\alpha = 5.2^\circ$, but none of these net models reached $F_i =$ 1.0 (100% F). The results also showed that the lowest F_i values were obtained for nets with high α (Fig. 9). The relationship F_i and α is somehow explained by the assumption that the filtration is evenly distributed over the net area and governed by the normal pressure drop and the tangential stress coefficient due to friction along the net wall. Gjøsund and Enerhaug (2010) showed how the tangential stress coefficient is likely to increase with increasing net panel roughness and decreasing Reynolds number, i.e., with increasing twine diameter and angle of attack (i.e., decreasing length of net) and decreasing velocity. Conical-shaped nets, such as those used in this study, are among the least efficient ($F_i = 0.75$–0.85), and they need to have high R_A (>3) to reach F_i < 0.9–0.95 values. Our results agree with this. The net with the lowest R_A (0.9) was associated with the lowest F_i (0.88) while net with the highest R_A (4.6) displayed the highest F_i (0.96) (Table 11 and Fig. 10). Further improvements in F_i and F_s can be obtained by using a porous cylindrical section ahead of the cone net (Currie, 1963; Smith et al., 1968). In this case, the water rejected by the tapering area of the cone can escape through the cylinder's mesh rather than out the mouth (Currie, 1963). This way of improving F_i is perhaps more relevant in large commercial trawls with changing taper angle than in small plankton nets.

In agreement with Gjøsund and Enerhaug, 2010, Enerhaug, 2005, our results demonstrated that F_i for typical plankton nets increased with increasing towing velocity and decreased with decreasing velocity (Fig. 8). Nets towed at very low speed (<0.5 ms^{-1}) filtered at a lower efficiency, but F_i increased with increasing towing speed. However, the effect plateaued at speeds >0.7–1.0 ms^{-1}. This positive correlation between F_i and U was contrary to common belief. As noted by Tranter and Heron (1967), there was a widespread and persistent, but incorrect, perception that F_i was generally negatively correlated with U, meaning that F_i decreased as towing velocity increased. Based on this belief, it is often recommended that plankton sampling nets should be towed at low velocities, and it was also assumed that a low towing velocity reduced clogging (Sournia, 1978). Our F_i results suggested that the tow speed of commercial fishing operations should be increased by 20% (from 0.5 to 0.6 ms^{-1} to 0.8–0.9 ms^{-1}). Despite the gains in F_i and reduced clogging by increasing U, the volume of water filtered by the trawl increased by approximately 20%. Because *Calanus* spp. are passively filtered by the net, increasing the volume of water filtered by the trawl should led to an increase in catch efficiency. However, this is a hypothetical situation for which the effect of clogging is widely unknown, and field testing to assess F_s is required to validate this hypothesis.

Over the course of a tow, clogging of particles (i.e., plankton, jellyfish) will reduce F_i. Reynolds (1969) suggested that the clogging rate may increase with decreasing tow velocity. Therefore, it is crucial to consider clogging with respect to filtered volume by the net and not with respect to tow time or distance covered (McQueen and Yan, 1993). Reduced clogging measured at low velocities may simply be due to filtering of less water and thus less plankton.

Finally, the effect of R_e on the C_D and F_i is not directly assessed in this study, but we are aware that different monofilament diameter d as those used in this study (198, 345, 318, 514 μm) may lead to different R_e. Thinner d leads to smaller R_e, which according to Breddermann (2017) lead to larger pressure loss coefficient and implies smaller F_i. To further understand the drag force dependency of the S_n and R_e and to be able to calculate it in an improved manner, it is necessary to understand the physics of the flow around the knot part of the net (Fredheim, 2006).

5. Conclusions

This study presented flow measurements through and forces on low porosity nets and provided simple expressions for the filtration efficiency and drag as functions of twine diameter, mesh opening, porosity, taper angle, and flow (towing) velocity. Our experiments using fine-meshed plankton nets showed good agreement between predicted and measured filtration efficiencies and demonstrated that the filtration efficiency for a square-meshed conical net increased with increasing velocity and porosity and decreasing netting angle to the flow. Hence, our measurements provided a reference for predicting the filtration efficiency of large commercial zooplankton trawls and understanding how it may vary with the towing velocity and the net parameters. Further tests assessing the effect of a porous cylindrical section ahead of the conical section are recommended. Likewise, field trials assessing filtration efficiency over prolonged tow times to account for clogging are needed to estimate the sustained filtration efficiency.

CRediT authorship contribution statement

Eduardo Grimaldo: Conceptualization, Data curation, Formal analysis, Funding acquisition, Investigation, Methodology, Project administration, Resources, Validation, Visualization, Writing – original draft, Writing – review & editing. **Bent Herrmann:** Conceptualization, Investigation, Writing – review & editing. **Enis N. Kostak:** Conceptualization, Investigation, Writing – review & editing. **Jesse Brinkhof:** Conceptualization, Investigation, Writing – review & editing.

Declaration of competing interest

The authors declare that they have no known competing financial interests or personal relationships that could have appeared to influence the work reported in this paper.

Data availability

Data will be made available on request.

Acknowledgments

Research Council of Norway through the Centre for Research-Based Innovation SFI-Harvest (Grant number 309661).

References

Aksnes, D.L., Blindheim, J., 1996. Circulation patterns in the North Atlantic and possible impact on population dynamics of *Calanus finmarchicus*. Ophelia 44 (1996), 7–28. https://doi.org/10.1080/00785326.1995.10429836.

Breddermann, K., 2017. Filtration Performance of Plankton Nets Used to Catch Micro- and Mesozooplankton: 2017,12 (Rostocker Meerestechnische Reihe) Paperback – 29 September 2017. ISBN-103844054057 :.

Costello, C., Cao, L., Gelcich, S., et al., 2020. The future of food from the sea. Nature 588 (2020), 95–100. https://doi.org/10.1038/s41586-020-2616-y.

Currie, R.I., 1963. The Indian Ocean standard net. Deep Sea Research 10 (1–2), 27–32.

Enerhaug, B., 2005. Flow through fine-meshed pelagic trawls. In: Lee, C.-W. (Ed.), Contributions on the Theory of Fishing Gears and Related Marine Systems, Proceedings of the DEMaT 2005, Busan, Korea, vol. 4, pp. 153–164. November 23–26, 2005.

FAO, 2020. The State of World Fisheries and Aquaculture 2020. Sustainability in Action. Rome. https://doi.org/10.4060/ca9229en.

Fredheim, A., 2006. Current Forces on Net Structures. Tapir Akademisk Forlag 2006 (ISBN 8247169991) 130 s. NTNU.

Gjøsund, S.H., Enerhaug, B., 2010. Flow through nets and trawls of low porosity. Ocean Eng. 37 (4), 345–354. https://doi.org/10.1016/j.oceaneng.2010.01.003.

Gjøsund, S., 2012. Simplified approximate expressions for the boundary layer Flow in cylindrical sections in plankton nets and trawls. Open J. Mar. Sci. 2 (2), 66–69. https://doi.org/10.4236/ojms.2012.22009, 2012.

Grimaldo, E., Gjøsund, S.H., 2012. Commercial exploitation of zooplankton in the Norwegian Sea. In: Ali, M. (Ed.), The Functioning of Ecosystems. 2012 Apr 27. InTechOpen, pp. 213–228. ISBM 978-953-51-0573-2.

Harris, R.P., Wiebe, P.H., Lenz, J., Skjoldal, H.R., Huntley, M. (Eds.), 2000. ICES Zooplankton Methodology Manual. Academic Press.

Hua, K., Cobcroft, J.M., Cole, A., Condon, K., Jerry, D.R., Mangott, A., Praeger, C., Vucko, M.J., Zeng, C., Zenger, K., Strugnell, J.M., 2019. The future of aquatic protein: implications for protein sources in aquaculture diets. One Earth 1 (3), 316–329. https://doi.org/10.1016/j.oneear.2019.10.018.

Larsen, T., 2009. Slepemotstand, Effektivitet Og Fangstsammensetning I Fiske Med Trål Tilpasset Dyreplankton. Forsøk Med Trål I Småskala. MSc thesis. The Norwegian College of Fishery Science, University of Tromsø. February 2009.

Lenihan-Geels, G., Bishop, K.S., Ferguson, L.R., 2013. Alternative sources of omega-3 fats: can we find a sustainable substitute for fish? Nutrients 5 (4), 1301–1315. https://doi.org/10.3390/nu5041301.

Liu, W., Tang, H., You, X., Dong, S., Xu, L., Hu, F., 2021. Effect of cutting ratio and catch on drag characteristics and fluttering motions of midwater trawl codend. J. Mar. Sci. Eng. 2021 (9), 256. https://doi.org/10.3390/jmse9030256.

McQueen, D.J., Yan, N.D., 1993. Metering filtration efficiency of freshwater zooplankton hausl: reminders from the past. J. Plankton Res. 15 (1), 57–65. https://doi.org/10.1007/BF00006688.

Nyatchouba Nsangue, B.T., Tang, H., Zhang, J., Liu, W., Xu, L., Hu, F., 2023. Experimental analysis of the influence of gear design and catch weight on the fluid–structure interaction of a flexible codend structure used in trawl fisheries. Appl. Sci. 2023 (13), 2505. https://doi.org/10.3390/app13042505.

Norwegian Directorate of Fisheries. Economic and biological figures from Norwegian fisheries 2022. https://www.fiskeridir.no/English/Fisheries/Statistics/Economic-and-biological-key-figures.

Nyatchouba Nsangue, B.T., Tang, H., Njomoue Pandong, A., Xu, L., Adekunle, D.M., Hu, F., 2022. Examining engineering performance of midwater trawl with different horizontal spread ratio, floatage, and weight parameters: a case study of model net for Antarctic krill fisheries. Int. J. Nav. Archit. Ocean Eng. 14 (2022), 100448 https://doi.org/10.1016/j.ijnaoe.2022.100448. ISSN 2092-6782.

Paschen, M., Winkel, H.-J., 2000. Flow investigations of net cones. In: Paschen, M., et al. (Eds.), Proceedings of the Fourth International Workshop on Methods for the Development and Evaluation of Maritime Technologies, Rostock 3-6 November 1999, vol. 1. Contributions on the Theory of Fishing Gears and Related Marine Systems, pp. 197–216.

Reynolds, A.J., 1969. Flow deflection by gauze screens. J. Mech. Eng. Sci. 11, 290–294. https://doi.org/10.1243/JMES_JOUR_1969_011_036_02.

Smith, P.E., Counts, R.C., Clutter, R.I., 1968. Changes infiltering efficiency of plankton nets due to clogging under tow. ICES J. Mar. Sci. 32 (2), 232–248. https://doi.org/10.1093/icesjms/32.2.232. November 1968.

Sournia, A. (Ed.), 1978. Phytoplankton Manual. UNESCO, Paris, 1978.

Tang, M.F., Dong, G.H., Xu, T.J., Zhao, Y.P., Bi, C.W., 2017. Numerical simulation of the drag force on the trawl net. Turk. J. Fish. Aquat. Sci. 17 (6), 1219–1230.

Tang, H., Hu, F., Xu, L., et al., 2019. Variations in hydrodynamic characteristics of netting panels with various twine materials, knot types, and weave patterns at small attack angles. Sci. Rep. 9 (2019), 1923. https://doi.org/10.1038/s41598-018-35907-1.

Thierry, N.N.B., Tang, H., Liuxiong, X., You, X., Hu, F., Achile, N.P., Kindong, R., 2020. Hydrodynamic performance of bottom trawls with different materials, mesh sizes, and twine thicknesses. Fish. Res. 2020 221, 105403. https://doi.org/10.1016/j.fishres.2019.105403.

Tranter, D.J., Heron, A.C., 1967. Experiments on filtration in plankton nets. Aust. J. Mar. Freshw. Res. 6, 281–291. https://doi.org/10.1071/MF9670089.

Valdemarsen, J.W., Øvredal, J.T., Åasen, A., Gjøsund, S.H., Hansen, K., 2011. Trålfangst: Årsaken til redusert effektivitet for enkelte tråltyper når fangsten øker. Sluttrapport til Fiskeri- og havbruksnæringens forskningsfond. Prosjekt 900285. Rapport fra Havforskningen Nr 2 (2011), 22. https://imr.brage.unit.no/imr-xmlui/handle/11250/116655.

Wan, R., Jia, M., Guan, Q., Huang, L., Cheng, H., Zhao, F., He, P., Hu, F., 2019. Hydrodynamic performance of a newly-designed Antarctic krill trawl using numerical simulation and physical modeling methods. Ocean Eng. 179 (2019), 173–179. https://doi.org/10.1016/j.oceaneng.2019.03.022. ISSN 0029-8018.

Zhou, C., Xu, L.X., Hu, F.X., Qu, X.Y., 2015. Hydrodynamic characteristics of knotless nylon netting normal to free stream and effect of inclination. Ocean Eng. 110 (2015), 89–97. https://doi.org/10.1016/j.oceaneng.2015.09.043.